Journal of Theoretical and Applied Information Technology
30th June 2020. Vol.98. No 12

ISSN: 1992-8645 www.jatit.org E-ISSN: 1817-3195

HOUSEBREAKING CRIME GAIT PATTERN CLASSIFICATION USING ARTIFICIAL NEURAL NETWORK AND SUPPORT VECTOR MACHINE

[1]HANA' ABD RAZAK, [2]ALI ABD ALMISREB, [1]MOHAMMED AHMED MOHAMMED SALEH & [1]NOORITAWATI MD TAHIR
[1]Faculty of Electrical Engineering, Universiti Teknologi MARA, Selangor, Malaysia
[2]International University of Sarajevo, 71210 Sarajevo, Bosnia and Herzegovina
Corresponding Author:nooritawati@ieee.org

ABSTRACT
The rate of crime is worsen and has led to a growing number of studies on human identification namely gait recognition. Hence, this study focused on the normal and anomalous behavior at the gate of residential units based on gait features extracted using Kinect sensor. Firstly, dataset of housebreaking crime behavior and normal behavior at the gate is acquired and collected. Further, orthogonal least squares (OLS) are utilized to extract and select the gait features along with principal component analysis (PCA) as gait feature optimization. Next, classification of gait features is done using artificial neural network (ANN) and support vector machine (SVM). Result attained showed that the recognition performance using ANN classifier was up to 99% but only 50% for SVM classifier. Findings from this study showed that the most optimum accuracy rate is at 99.78% using ANN with GDX as the learning algorithm in classifying both normal and anomalous behavior at the residential gate units.
Keywords: *Anomalous Behavior, Kinect, Orthogonal Least Square (OLS), Principal Component Analysis (PCA), Artificial Neural Network (ANN), Support Vector Machine (SVM)*

1. INTRODUCTION

There are millions of anomalous behaviors that can be investigated and analyzed as fulfilling the requirement in creating a safe and secure world. Therefore enormous studies are conducted in analyzing the human behavior either normal or anomalous using machine learning algorithms in combination with gait biometric. Currently, studies on anomalous gait behavior can be divided into three categories, i) health, ii) suspicious and iii) crime. Previously, studies on anomalous gait behavior of the health category include care for the elderly and detecting adverse behavior in human posture. Basically, studies on anomalous gait behavior of the suspicious category focus on the negligence in human behavior that leads to awkward situations. Finally, studies on the anomalous gait behavior of crime category emphasize violent acts that could pose a threat or danger to the people.

2. RELATED WORKS

The health category studies are mostly focused on monitoring the daily activities of the elderly at their home or home care through surveillance systems. These systems should be able to be used for detection of wandering and falling behavior among the elderly [1][2]. Health category also engaged studies related to body postures that address the risk of occupational musculoskeletal disease due to unhealthy sitting postures [3] and the risk of neck pain usually contributed by Computer Vision Syndrome [4]. This syndrome is often caused by the extreme usage of computer and smartphone.

Conversely, suspicious category is the most popular studies in anomalous gait behavior that includes wrong direction, wrong place, driving behavior and crowd anomaly. Wrong direction studies are interested in pedestrian behavior in public places [5]. Studies of wrong place are for detecting human that move towards the unsafe places such as 'trackbed' region of the train, loitering, entering from exit passage, including studies of the abandoned object at public places [5]–[7]. Driving behavior can be associated with anomalous behavior if the subject(s) are detected texting, talking on the phone, gaming, eating, drinking, putting on cosmetics during driving [8], [9]. On the other hand, the crime category involved violent behavior against people in two places, for instance, public area and specific venues such as automated teller machines (ATMs), elevators and residential homes. The violent behavior is considered to distinguish and consistent as compared to normal behavior, therefore, the postures that are detected differently from normal

ISSN: 1992-8645 www.jatit.org E-ISSN: 1817-3195

behavior are identified as anomalous. This idea is applied in detecting the anomalous behaviors of crime category in public areas including postures of pointing, punching, kicking, street fighting, smashing cars and robbery [7], [10]–[12]. The aggressiveness, fiddling, peeping, and squatting are the anomalous postures at the ATMs and elevators [13]–[15].

On the contrary, machine learning algorithms view an image as an object that made up of thousands or even millions of pixels. Mathematically, these millions of numerical values of the pixels are represented as feature vectors to enable machine learning to understand the pattern of the image. Traditionally, two stages are essential for machine learning algorithms to achieve better performance namely feature extraction and classification. The best features of the image are selected through feature extraction methods along with the best tuning classifier parameters for classification. Prior to these two stages, the pre-processing image is vital to generate the region of interest for feature extraction and classification process. The detection of a moving region of an image can be achieved using several methods, for instance background subtraction, statistical method, temporal differencing and optical flow [16]. The optimization can be implemented using shadow detection, images morphological such as erosion and dilation and many more [17].

Nowadays, motion caption (Mocap) data can help to avoid the hassle of pre-processing images. It provides 3D skeletal data from the human body that can be exploited to simulate complex motions. Mocap data can be generated either using markers or markerless. Mocap data with markers are captured by the Mocap system that consists of multiple high-resolution infrared cameras along with multiple reflective markers. Markerless mocap data can be captured using the markerless mocap systems or Microsoft Kinect (Kinect) for Xbox 360. The marker or markerless 3D skeletal data captured by the mocap system is specific, accurate and stable but it comes at a high cost. Kinect offers an alternative for capturing reliable markerless data and at low cost. It can automatically generate 20 skeleton joints together with vector data of each joint and it excludes the background of the images referring to the surrounding of the event or the designated space for the performance.

The study by W. Zhang et al. [18] in 2013 identified anomalous behavior using static and dynamic features of 15 body joints on the Z-plane of Kinect during dim environment representing evening time. Hand joint has been excluded due to occlusion and is usually beyond the measurable range of Kinect which can measure only 57 degrees. Static features are height, length, hand-span, arm span, whilst dynamic features include body parts movement for instance hand movement, leg movement and many more. The approach of this study was to compare the anthropometric data of the household with outsiders in determining the intruders. Classification of the intruder used 10-fold cross-validation artificial neural network (ANN) with a learning rate of 0.1 and 300 epochs of learning. The average classification rate was 94%. In 2015, the anthropometric measurements and gait data were applied in gait recognition using 20 body joints of varying heights, weights and clothing. The anthropometric measurements include height and length. The height of the body is calculated from the target joints to the ground such as the full-body, torso and lower limb as well as length is the distance between left and right joints. The classification utilized three classifiers namely ANN, k-nearest neighbors (kNN) and support vector machine (SVM). The accuracy of the gait cycle was lower than the accuracy of anthropometric measurements for all three classifiers. The highest accuracy of gait cycles was 63% with SVM classifier and the highest accuracy of anthropometric measurements was 85% with kNN classifier [19]. Two studies employed SVM classifier, multi-person gait recognition and gesture recognition. Recognition of multi-person included several environments, clothing and footwear from 14 body joints and excluding the joints of the arm and hand. Principal Component Analysis (PCA) was used for feature extraction and feature identification used SVM classifier. This approach attained 100% accuracy rate in identifying people from their walking patterns [20]. The angle and velocity of 20 body joints were calculated and classified using SVM with radial basis function (RBF) kernel and relevance vector machine (RVM) with Bayesian frameworks to distinguish human gestures. Joint angles were measured from 35 angles of arm, leg and center body joints. Meanwhile, angle velocity was the difference between angles in two frames. The γ parameter of SVM and RVM was varied from 2-15 to 210 and regularization parameter C of SVM was fixed at 1. Gesture classification with SVM acquired slightly lower error rates than RVM by 8% and 9%, respectively [21]. In 2018, N. Khamsemanan et al. [22] have proposed gait recognition using posture-based from four body joints i.e. hip-center, hip-left, hip-right, and spine according to the dimensions and positions of the body parts. The classification employed three learning algorithms namely kNN, ExtraTrees and

multiple layer perceptron (MLP). The highest accuracy of 97% was obtained using MLP classifier. Recently, E. Owaidah et al. [23] have discovered three distinctive joints namely spine-center, shoulder-left and shoulder-center in recognition of the wearer of the loose garments that conceal most of the body joints. Gait features on Y-plane of Kinect are used as features by detecting the position of the body joints. The joints were classified using KNN and the recognition accuracy was up to 83%.

Inspired by diverse studies in gait recognition using mocap data, we investigated two machine learning algorithms specifically ANN and SVM in detecting normal and anomalous behavior at the gate of residential units. Firstly, two types of behavior at the residential unit gate are determined namely normal and anomalous. Both normal and anomalous behaviors are identified for several activities associated with residential unit gate and housebreaking crime. Gait features of skeleton joints are acquired using Kinect. Next, these gait features are extracted using orthogonal least square (OLS) algorithm. Further, these gait features are optimized using PCA prior to classification using 10-fold cross-validation for both ANN and SVM classifiers. This paper is organized as follows; Section 1 presented the introduction of anomalous behavior and previous researches related to gait recognition. Next, Section 2 explained the theories of each algorithm used in this study namely OLS, PCA, ANN, and SVM. Section 3 detailed the proposed methodology along with data collection followed by feature extraction, feature selection, optimization followed by classification. Discussion on experimental analysis and results are given in Section 4. Finally Section 5 concludes our findings.

3. THEORETICAL PARADIGM

This section presents the theories of feature extraction algorithms specifically OLS and PCA followed by the classification using ANN and SVM.

3.1 Orthogonal Least Squares (OLS)

The least squares method is appropriate to avoid the curse of dimensionality by minimizing the sum of squares error function [24], [25]. The orthogonal least squares measures both errors in abscissa and ordinate values to minimize the sum of squares error of orthogonal distance between the data and the line.

The least squares method can be interpreted through the geometric relationship among parameters that orthogonally projected onto span*(A)* as shown in Figure 1.

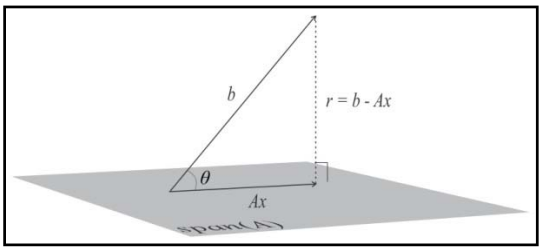

Figure 1: Geometric Interpretation of Least Squares Method

Clearly, vector Ax is the orthogonal projection of b onto span*(A)*,

$$Ax \approx b \quad (1)$$

Then, error r is orthogonal onto span*(A)*

$$r = b - Ax \perp span(A) \quad (2)$$

The sum of squares errors can be written as $\sum_{i=1} r_i^2$ and the minimum condition of orthogonal least squares can be concluded as,

$$\min_x \|b-Ax\| \quad (3)$$

A memory-efficient algorithm with numerically robust transformation that yields computational problem is necessary that involves high dimensional data. The most important aspect is not changing or losing too much information of the data. To do so, the QR factorization is applied to matrix A with $A = QR$.

Recall :
$$\begin{aligned} Ax &\approx b \\ QRx &= b \\ Rx &= Q^T b \end{aligned}$$

The matrix $Q \in \mathbb{R}^{m \times n}$ is orthogonal to $R \in \mathbb{R}^{n \times n}$ and is an upper Hessenberg matrix. The Householder transformation of QR factorization is used for constructing stable matrix transformation. The Householder algorithm generates R-factor of QR factorization and Householder vectors.

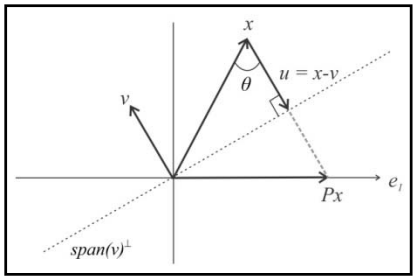

Figure 2: Householder Transformation

ISSN: 1992-8645 www.jatit.org E-ISSN: 1817-3195

A Householder transformation is a reflection across the plane perpendicular to a unit vector v as in Figure 2. It has real orthogonal matrices of the form,

$$H = \beta v v^T, \quad \beta = \frac{2}{v^T v} \tag{4}$$

Householder matrix is symmetric, orthogonal and unitary where v is Householder vector that associated with Householder matrix.

$$Q = H_1,\ldots,H_n, \quad H_i \in \mathbb{R}^{m \times m} \tag{5}$$

For any arbitrary vector $x \in \mathbb{R}^n$, $x \neq 0$, , the Householder matrix can be written as:

$$Hx = \left(I - \beta v v^T\right)x \tag{6}$$

and the vector can be defined specifically as:

$$u = x - \|x\| e_1 \tag{7}$$

If x is reflected onto identity plane e_1, a matrix of rank 1, the reflection of vector x is zeros out all elements except for the first element. Hence a sequence of the Householder matrix can be applied to zero components of a vector.

$$H\begin{bmatrix} x_1 \\ \vdots \\ x_n \end{bmatrix} = \|x\| \begin{bmatrix} 1 \\ \vdots \\ 0 \end{bmatrix}$$

$$Hx = I - \beta v v^T \tag{8}$$

This leads to the development of R-factor of QR factorization. This transformation is less complex since it requires only a unit vector, v instead of a full matrix, H.

3.2 Principal Component Analysis (PCA)

PCA is a tool for determining patterns in high dimensional data, $A \in \mathbb{R}^{n \times d}$ by finding the new representation of A, $X \in \mathbb{R}^{n \times k}$ where $k \leq d$. Mathematically, principal components can be derived by maximizing the variance to find new representation without losing much information.

Applying the spectral theorem, let ϕ be a linear map for the input vector, v_i. X is a real number matrix, $X \in \mathbb{R}^{n \times k}$ and the transpose matrix of A is A^T. Since $A=A^T$ is symmetric, the matrix is orthogonally diagonalizable and consists of solely real eigenvalue. Let $\{v_1, v_2, \ldots, v_n\}$ be an orthogonal non-zero vector in A for each $i = 1, 2, \ldots, n$. Thus, ϕ can be written as follows,

$$\phi : Av_i = \lambda v_i \tag{9}$$

Statistically, for a single variable of X, the mean can be calculated as,

$$\mu_x = \frac{1}{n}\sum_{i=1}^{n} x_n \tag{10}$$

and the variance for a single variable of X,

$$var(x) = \frac{1}{n-1}\sum_{i=1}^{n}\left(x_n - \mu_x\right)^2 \tag{11}$$

Further the covariance of two variables x and y of X can be defined as,

$$cov(x,y) = \frac{1}{n-1}\sum_{i=1}^{n}\left(x_n - \mu_x\right)\left(y_n - \mu_y\right) \tag{12}$$

When α data vectors of n×1 matrix, $\alpha \in \mathbb{R}^n$ is juxtaposed into a matrix, X, the projections can be presented as $x\alpha$. The variance can be acquired using Equation (11 as follows [26], [27],

$$\begin{aligned} var(\alpha) &= var(\alpha) = \frac{1}{n}\sum_{i=1}^{k}\left(x_n \cdot \alpha\right)^2 \\ &= \frac{1}{n}\left(x_k\alpha_k\right)^{\mathrm{T}}\left(x_k\alpha_k\right) \\ &= \frac{1}{n}x_k{}^T\alpha_k{}^T x_k\alpha_k \\ &= \alpha_k{}^T\alpha_k\frac{x_k{}^T x_k}{n} \\ &= \alpha_k{}^T\alpha_k V \end{aligned} \tag{13}$$

Spectral theorem allows the utilization of covariance matrix V in finding eigenvector due to its properties of having prominent eigenvalues by maximizing the variance. The maximization is restricted at unit vectors by applying the constraint, $C = \alpha_k{}^T\alpha_k - 1$ $C = \alpha_k\alpha_k - 1$ or.

$$var(\alpha)_{max} = \alpha_k{}^T\alpha_k V - C \tag{14}$$

Thus, eigenvectors and eigenvalues can be derived by multiplying the new variable of Lagrange multiplier, λ with the C, and differentiate the function with respect to α and λ,

$$\mathcal{L}(\alpha,\lambda) = \left(\alpha_k{}^T\alpha_k V\right) - \lambda\left(\alpha_k{}^T\alpha_k - 1\right) \tag{15}$$

$$\frac{\partial\mathcal{L}}{\partial\lambda} = \alpha_k{}^T\alpha_k - 1 \tag{16}$$

$$\frac{\partial\mathcal{L}}{\partial\alpha} = \alpha_k{}^T V - \lambda\alpha_k{}^T \tag{17}$$

ISSN: 1992-8645 www.jatit.org E-ISSN: 1817-3195

Then, the derivatives are setting at the optimum condition which is zero.

$$\alpha_k{}^T \alpha_k = 1 \quad (18)$$

$$\alpha_k{}^T V = \lambda \alpha_k{}^T \quad (19)$$

Equation (18) and (19) notify that λ is the eigenvalues and $\alpha_k{}^T$ is an eigenvector of the covariance matrix, V.

The earlier derivation is respecting the spectral theorem and yielded the covariance matrix, V, the eigenvectors are orthogonal to each other so the projection of $\alpha_{k+1}{}^T$ is uncorrelated to $\alpha_k{}^T$, and the eigenvalues must be ≥ 0.

3.3 Artificial Neural Network (ANN)

ANN is a mathematically computational model inspired by the competency of biological neuron in the human brain. The hallmark of ANN lies within its capability to learn and apply the knowledge of a pattern. Multi-layer perceptron (MLP) is a standard ANN model consisting of networks with three or more parallel layers; input layer, hidden layer, and output layer.

In this network, the knowledge is learned through its parallel weights as in Figure 3. In the learning process, weights are adjusted according to the output of the layers and the errors are propagated backward as in (20). The learning process can be optimized by minimizing errors based on the optimization function. The objective of backpropagation is to reduce the errors until the network achieved the knowledge to be learned. Then, weights are calculated using the non-linear activation function to propagate to the next layer. Regularly, learning process of MLP adopts the gradient descent algorithms as the optimization function [28][29][16], mean square error (MSE) [29] as the performance function and sigmoid [30][16] as the non-linear activation function.

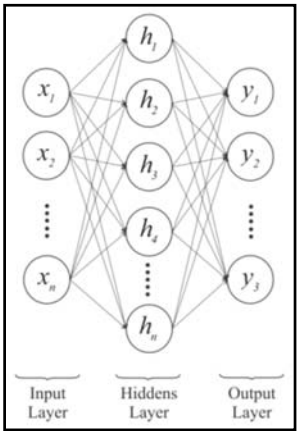

Figure.3: Multi-Layer Perceptron Architecture of ANN

$$x: (W, b) = \varphi(W \cdot x + b) \quad (20)$$

3.4 Support Vector Machine (SVM)

SVM is a linear model for binary classification. It attempts to separate sets of data in the feature space at the optimal margin by creating a hyperplane. The optimal hyperplane can be obtained by balancing the margin maximization using regularization parameter, C. It is crucial to correctly tune C to ensure that the margins are well separated between the data. If C value is too large or too small, the classification process may lead to overfitting or misclassification. SVM can solve linear and non-linear data. Non-linear data are represented as a linear function in a higher-dimensional space. The non-linear space can be defined by the kernel function. Three most common kernel functions include linear, radial basis function (RBF) and polynomial [30]. Each kernel has different parameters to configure specifically C for the linear kernel, γ for RBF kernel and degree, d for the polynomial kernel. Figure 4 showed the learning process in SVM. SVM can solve linear and non-linear data. Non-linear data are represented as a linear function in a higher-dimensional space. The non-linear space can be defined by the kernel function. Three most common kernel functions include linear, radial basis function (RBF) and polynomial [31]. Each kernel has different parameters to configure specifically C for the linear kernel, γ for RBF kernel and degree, d for the polynomial kernel.

ISSN: 1992-8645 www.jatit.org E-ISSN: 1817-3195

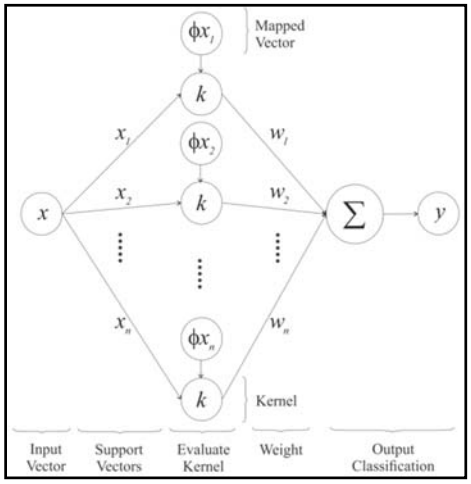

Figure.4: The Architecture of SVM

The linear kernel can be defined as in ((21),

$$K\left(x_i, x_j\right) = x_i \cdot x_j \quad (21)$$

The RBF kernel is extensively utilized for classification of anomalous gait behavior due to better accuracy [32]–[34] The function can be expressed as in ((22),

$$K\left(x_i, x_j\right) = e^{\frac{-\left\|x_i - x_j\right\|^2}{2\gamma^2}} \quad (22)$$

The function of the polynomial kernel is as outline in (23),

$$K\left(x_i, x_j\right) = \left(x_i \cdot x_j + 1\right)^d \quad (23)$$

4. PROPOSED METHODOLOGY

This section discussed in detail the methodology used in this study. First is the data collection of both normal and anomalous behavior. Next is feature extraction and feature selection using OLS along with feature optimization using PCA and finally is the classification stage using ANN and SVM as classifiers

4.1 Data collection

The data collection process was done according to the definition of housebreaking crime behavior by the Royal Malaysia Police (RMP). Anomalous gait is referring to the combination of any three anomalous gait postures (bending, squatting and kneeling) that were performed sequentially or repeatedly in any order in front of residential unit. Participants were not guided to act exactly as the perpetrator of housebreaking crime, however, they were encouraged to imagine as one. This is to ensure the authenticity of the collected data. A multi-condition gate was provided in the laboratory with a Kinect mounted on a 2.3-meter ladder at a distance of 3 to 3.3 meters between the gate and the camera. This is the best setting of Kinect camera for tracking participants' images by adhering to the practical ranging limit of the camera and mimicking the installation of CCTV camera in most residential units. Next, motion data were recorded using Kinect.

Prior to the data collection process, detailed observation and investigation have been carried out on the datasets provided by the online motion capture database such as CMU Graphic Lab, Mocap database HDM05, UTD-MHAD dataset, Emotional Body Motion Database and the largest database, Eyes, Japan. It is to ensure that the collected data correspond to the standard data utilized by previous researchers. From the investigations, the standard datasets of motion capture database hold similar properties as; (i) the actions are performed without using the actual tool(s), (ii) the participants perform a pantomime referring to specific behavior of humans or animals according to the requirement of the study, (iii) the participants act the movements repeatedly with slight adjustment, (iv) the architecture of the recording site must imitate the actual place and (v) the length of data taken depends on the scenarios [35]–[39]. Figure 5(a) showed the skeleton images of normal activities such as unlocking the padlock or latch, taking brochures, picking up items from the ground and giving direction whilst Figure 5 (b) showed some images of housebreaking crimes including lurking and sneaking activities.

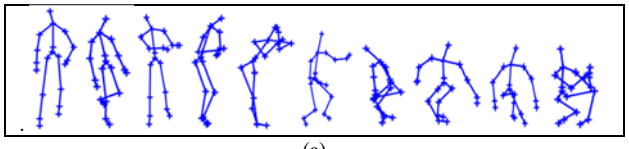

(a)

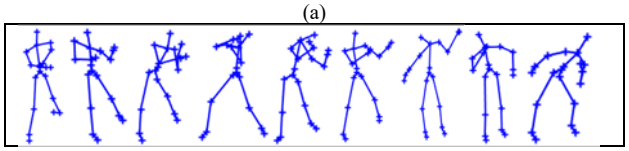

b(i)

Journal of Theoretical and Applied Information Technology
30th June 2020. Vol.98. No 12

ISSN: 1992-8645 www.jatit.org E-ISSN: 1817-3195

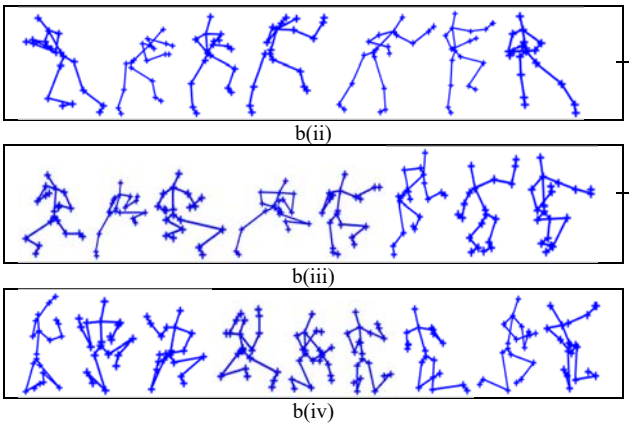

Figure 5: Input Images of Features Analysis, (a) Body Posture of Normal Behavior, (b) Body Posture of Anomalous Behavior, (i) Standing, (ii) Bending, (iii) Squatting, and (iv) Kneeling

4.2 Feature Extraction and Feature Optimization of Anomalous Gait

The process of gait features data arrangement began by removing the untracked frames to ensure the validity of the dataset. The untracked frames could be generated by Kinect if the image is out of range, heavy occlusion or if the movements are too fast. In this study, a total of 223 scenes of normal motion and 236 scenes of anomalous motion were captured and acquired. Each scene contains 1400 gait features that were yielded from 35 frames along with 20 body joints of Kinect on 2-plane of X-plane and Y-plane. Next, OLS was employed to extract and select the most effected joints during normal and anomalous activities at the gate of the residential unit. The size of gait features during normal activities and anomalous activities were 1400 by 223 and 1400 by 236 gait features respectively. Further, these features were resized to 1400 by 459 and set as two classes, with both normal and anomalous data arranged together in determining the most effected joints during both activities. Further, PCA was employed to optimize the selection of features obtained by OLS due to the close relationship between OLS and PCA [40] and its ability in extracting the best gait features while preserving the information of the data. The pseudo-code of PCA is as shown in Table 1.

Table 1: Algorithm for Optimizing the Features of Anomalous Gait Language

Input	:	$A \in \mathbb{R}^{d \times n}$	Total	:	$A \in \mathbb{R}^{840 \times 459}$
Output	:	$\alpha_k^T \in \mathbb{R}^{n \times k}$	(Eigenvector)		
	:	$\lambda \in \mathbb{R}^{n \times k}$	(Eigenvalues)		

1: Load and transpose A, $A^T \in \mathbb{R}^{n \times d}$
2: Normalize A^T, $\mu = 0$, $\sigma = 1$
3: Re-centered A^T
4: Write the centered data in a symmetric matrix, $X^T X = v_i X$
5: **for** t < n
6: Calculate the variance of $X \in \mathbb{R}^{n \times k}$ for $k=1,2,\ldots,n$, $var\left[\alpha_k x, |\alpha_k x\right] = \alpha_k{}^T \alpha_k V$
7: Utilize the covariance matrix, $V \in \mathbb{R}^{n \times n}$ to find the eigenvectors
8: Maximize the variance at unit vector with the constraint, C
9: Add new variable using Lagrange multiplier, λ to the function
10: Differentiate the function with respect to α and λ at the optimum condition
11: Obtaining the eigenvectors, $\alpha_k{}^T$ and eigenvalues, λ of V
12: **end for** t
13: Arrange $\alpha_k{}^T$ according to the values of λ in descending order
14: Output, $\alpha_k{}^T$, and λ

The first principal component (PC) is the eigenvector with the largest value of eigenvalues and the ranking is descending according to the eigenvalues. There are several criterion in selecting the significant PCs that contain the most useful information of original data from the new representation of data upon completion of PCA [41], [42]. In this study, the cumulative percentage of variance, criterion of eigenvalue and criterion of the scree plot were used in determining the significant PCs.

4.3 Anomalous Gait Classification

Artificial neural network (ANN) and support vector machine (SVM) acted as classifiers in classifying normal and anomalous behavior during housebreaking crimes. The architecture of both classifiers was tuned according to the network parameters of both algorithms.

A three layers multi-layer perceptron (MPL) of ANN was used for this purpose. Four training algorithms were evaluated and validated for classification purpose namely:

- scaled conjugate gradient (SCG);

ISSN: 1992-8645 www.jatit.org E-ISSN: 1817-3195

- gradient descent with adaptive learning rate (GDA);
- gradient descent with momentum (GDM) and
- gradient descent with momentum and adaptive LR (GDX).

Input features of the networks consist of 459 scenes. The sampling data used was 10-fold cross-validation technique. The learning process was repeated for 10 times for different sets of training and testing data. Therefore, each process used 413 scenes for training and 46 scenes for testing. The input features or weights were normalized in the range of -1 to +1 using hyperbolic tangent activation function to transfer the weights from the hidden layer to the output layer. Then, the softmax activation function calculated the probability of each weight and cross-entropy was compared for the probability of the weights with the output. The hidden layer was varied from 10 to 100 and the initial weight from 1000 to 10000. Table 22 tabulated the proposed architecture of ANN used in this study whilst Table 3 listed the three types of kernel used by the SVM classifier. Classification with linear kernel involved the regularization parameter *C* for all kernels. Parameter *C* was varied with certain range to determine the best value in separating the feature vectors. RBF kernel required the variation of parameter γ in order to adjust the curvature of decision boundary correctly. The polynomial kernel is by varying parameter *d* to identify the best location of hyperplane to separate the features. Table 3 presented the parameters used in each SVM kernel.

Table 2: Architecture of ANN

Parameter	Type / Size
Learning Algorithm	SCG, GDA.GDM and GDX
Epoch	1000
Learning rate	0.01 (GDA, GDM, GDX)
Momentum	0.9 (GDM, GDX)
Validation frequency	7
Activation function in hidden layer	Hyperbolic tangent sigmoid
Activation function in output layer	Softmax
Performance function	Cross-entropy

Table 3: Architecture of SVM

Kernel	Parameter	Size
Linear	*C*	1 to 1000
RBF	*C*	10 to 1000
	γ	0.01 to 1
Poly	*C*	0.01 to 10
	d	3 to 5

5. RESULTS AND DISCUSSION

This section analyzes the significant joints and significant features of normal and anomalous gait obtained from OLS and PCA. The validation of normal and anomalous behavior is acquired from the classification process using ANN and SVM classifiers.

5.1 Analysis of Significant Joints of Normal and Anomalous Gait using OLS

In this section, the results attained using OLS for extracting significant features of both normal and anomalous behaviors at the gate of the residential unit is elaborated. Table 4 showed the comparison between the original 40 joints of Kinect as compared to OLS selection towards significance skeleton joints during activities at the gate. The ranking was determined by the average error. Note that skeleton joints with higher average error are more significant. From the results attained, the first 20 ranks were dominated by skeleton joints of X-plane except the 7th, 11th and 13th rank occupied by the center joints of Y-plane. This implied that skeleton joints of X-plane were more significant.

Further, analyzing the OLS selection rank, the first 20 joints are the torso body joints except for five lower body joints at 12th, 15th, 17th, 18th and 20th rank. In this study, torso body joints are referred as head, spine, center hip, shoulder, elbow, wrist, and hand. The lower body joints are referred as left hips, right hips, knee, ankle, and foot. These 20 joints resembled the normal and anomalous behaviors based on Kinect skeleton joint structure. The rest of the joints were scattered and could not be interpreted according to the skeleton joint structure as in Figure 6.

The selection of significant skeleton joints was performed using four training algorithms of ANN and three kernels of SVM as shown in Figure 7 and Figure 8 respectively. The joints were classified in increment of two therefore 20 combinations of skeleton joints were conducted for 40 skeleton joints.

Refer to Figure 7 and Figure 8, ANN classifier with all for learning algorithms namely SCG, GDA, GDM and GDX have proven suitable in recognizing the difference between normal and anomalous behavior. The 12th set of OLS selection with 24 skeleton joints recorded highest sensitivity and specificity and these two performance measures are consistent for all ANN classifiers based on the four learning algorithms. In addition, the 14th, 16th till the 20th sets also showed highest sensitivity using ANN-GDX classifier as depicted in Figure 7. This

ISSN: 1992-8645 www.jatit.org E-ISSN: 1817-3195

resembled the classifier ability to identify anomalous gait as 'anomaly'. Further in Figure 8, highest specificity at 100% is at 20th set once again with ANN-GDX.

This indicated the classifier ability in identifying normal gait as 'normal'. Further, to determine the most significant joints during normal and anomalous behaviors, the OLS selection rank were compared with Kinect body joint. Skeleton joints of the 12th set contained some similarity with the postures of anomalous gait. The 14th, 16th through 20th sets were discovered to be scattered and cannot be related to the postures of anomalous gait.

Table 4: Forty Skeleton Joints according to Kinect Body Structure and OLS Selection Rank

Kinect Body Structure		OLS Selection Rank		
Kinect Joint	**Joint Name**	**Kinect Joint**	**Joint Name**	**Average Error**
1	Hip CX	4	Head CX	0.2789
2	Spine CX	3	Shoulder CX	0.1416
3	Shoulder CX	5	Shoulder LX	0.0860
4	Head CX	2	Spine CX	0.0615
5	Shoulder LX	6	Elbow LX	0.0613
6	Elbow LX	1	Hip CX	0.0603
7	Wrist LX	21	Hip CY	0.0415
8	Hand LX	12	Head RX	0.0325
9	Shoulder RX	8	Hand LX	0.0210
10	Elbow RX	7	Wrist LX	0.0197
11	Wrist RX	22	Spine CY	0.0172
12	Hand RX	16	Foot LX	0.0168
13	Hip LX	23	Shoulder CY	0.0135
14	Knee LX	11	Wrist RX	0.0097
15	Ankle LX	15	Ankle LX	0.0078
16	Foot LX	9	Shoulder RX	0.0072
17	Hip RX	17	Hip RX	0.0059
18	Knee RX	13	Hip LX	0.0058
19	Ankle RX	10	Elbow RX	0.0058
20	Foot RX	20	Foot RX	0.0055
21	Hip CY	24	Head CY	0.0045
22	Spine CY	14	Knee LX	0.0045
23	Shoulder CY	19	Ankle RX	0.0036
24	Head CY	25	Shoulder LY	0.0033
25	Shoulder LY	30	Elbow RY	0.0030
26	Elbow LY	18	Knee RX	0.0029
27	Wrist LY	26	Elbow YL	0.0028
28	Hand LY	32	Hand RY	0.0024
29	Shoulder RY	29	Shoulder RY	0.0023
30	Elbow RY	33	Hip LY	0.0021
31	Wrist RY	36	Foot LY	0.0013
32	Hip LY	28	Hand LY	0.0011
33	Knee LY	38	Knee RY	0.0011
34	Ankle LY	27	Wrist LY	0.0010
35	Foot LY	35	Ankle LY	0.0010
36	Hip RY	37	Hip RY	0.0009
37	Knee RY	40	Foot RY	0.0008
38	Ankle RY	31	Wrist RY	0.0007
39	Foot RY	34	Knee LY	0.0007
40	Hip LY	39	Ankle RY	0.0006

Note. L signifies left body joint, R signifies right body joint, X signifies X-plane and Y signifies Y-plane

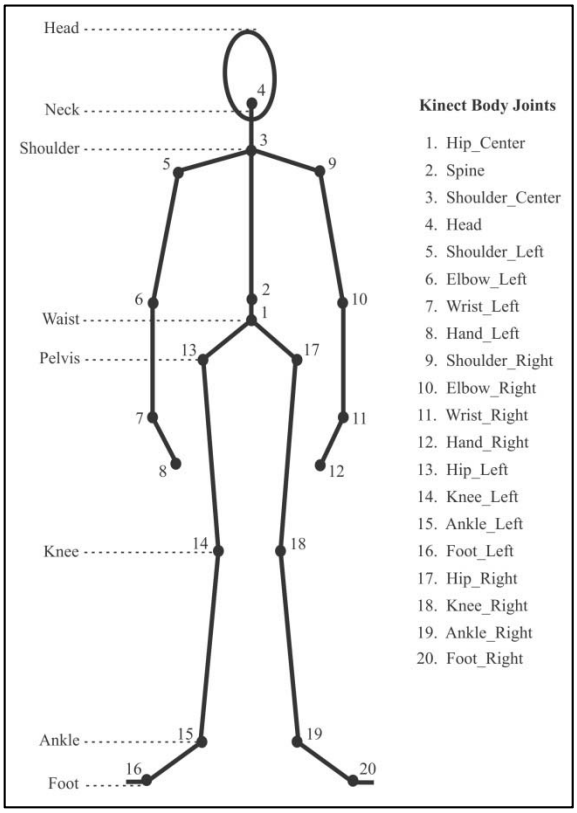

Figure 6: Body Joint Structure of Kinect

Therefore, these skeleton joints were excluded from the optimization process. This portrayed that the 12th set contained the most significant features of anomalous gait according to the OLS ranking with high sensitivity.

Skeleton joints of the 12th set also complied or fulfilled the definition of anomalous gait by RMP. Thus, this set was selected as the optimized set using PCA in determining the significant features of skeleton joints of the postures. OLS with ANN classifiers has successfully propounded a relationship between skeleton joints during normal and anomalous activities according to the 24 selected joints. Ten anthropometric traits can be extracted from the 24 selected joints namely head, shoulder, spine, elbow, hip, hand, wrist, foot, ankle, and knee. Obviously, normal and anomalous behaviors shared similar postures during activities at the residential gate.

Journal of Theoretical and Applied Information Technology
30th June 2020. Vol.98. No 12

ISSN: 1992-8645 www.jatit.org E-ISSN: 1817-3195

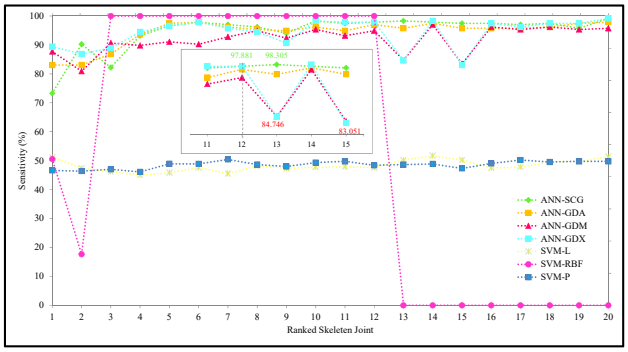

Figure.7: Sensitivity of Twenty Combinations of Skeleton Joints Based On OLS Selection Rank

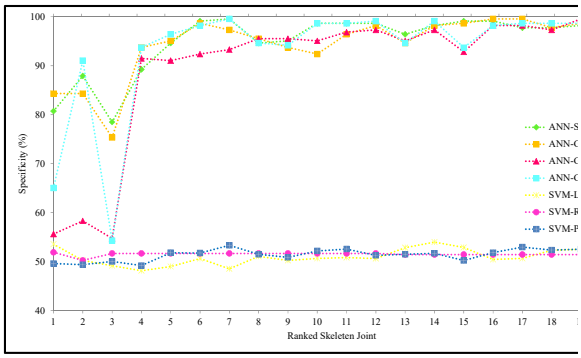

Figure.8: Specificity of Twenty Combinations of Skeleton Joints Based On OLS Selection Rank

5.2 Significant Features of Normal and Anomalous Gait using PCA

Twelfth set of OLS selection rank with total size of 840 by 459 gait features was transformed to orthogonal linear space using PCA. As mention earlier, the three PCA rules of thumbs:

- Eigenvalue Criterion (EoC);
- Scree Test and
- Cumulative (Cum) percentage of variance

were used in determining the significant PCs of gait features. For EoC, PCs with eigenvalues greater than unity (>1) were preserved. Next, for Scree plot the criteria are to preserve PCs that stabilized in variation of data. Finally, PCs with cumulative percentage of the variance between 80% - 99% can be extracted and sufficient to be preserved and these can be used to represent the significant information of the original data.

Upon completion of the experimental analysis it was found that for EoC, out of 1400 feature vectors, 458 eigenvalues are greater than one. Secondly for Scree Test, as depicted in Figure 9 five PCs were chosen based on the Scree plot. Further, Figure 10 showed that for cumulative percentage of variance, it was found that 97% - 99% are indeed apt to be chosen as the range to be preserved. The number of PCs is 80 PCs at 97%, 114 PCs at 98% and 177 PCs at 99% respectively. Next each of these PCs acted as inputs to both ANN and SVM classifiers.

The classification results using both ANN and SVM classifiers are as tabulated in Table 5. Overall, it is observed that the difference in classification rate between ANN classifier and SVM classifier are drastic. Highest accuracy (Acc) attained in classifying normal and anomalous behavior with ANN-GDX is 99.78 whilst with SVM the highest accuracy was only 51.85% with linear and RBF kernels. Further, with Cumulative Variance, accuracy of ANN classifier based on several learning algorithms was consistent specifically above 97% except for ANN-GDM. As for SVM classifier, all three kernels showed poor accuracies since SVM only achieved accuracy between 49% - 51.85%. In addition, similar accuracy performances are observed for SVM classifier with PCs extracted from Scree and EoC as inputs as well. Conversely, PCs extracted using Scree plots as inputs to ANN classifier, performed higher as compared to SVM, however the accuracy attained is lower as compared to Cumulative variance as inputs to ANN classifier.

Note that for ANN classifier, PCs extracted from EoC showed lowest accuracy rate for all learning algorithms except for ANN-SCG but the accuracy rate is still lower than 90%. As for sensitivity (Sens), ANN-GDA and ANN-GDX outperformed others with perfect rate using 97% Cumulative Variance as compared to Scree Test and EoC.

This showed the classifiers ability to identify anomalous behavior as ‘anomaly’ is at 100% performance by both ANN-GDA and ANN-GDX as well. As for specificity (Spec), once again ANN-GDX showed highest rate specifically 99.55% at Cumulative Variance of 97% in identifying normal behavior as ‘normal’. As expected, SVM with all three kernels showed poor sensitivity and specificity results since the accuracy rates attained are not encouraging. Results obtained showed that ANN-GDX is the best option in classifying anomaly behavior gait for residential unit based on accuracy,

Journal of Theoretical and Applied Information Technology
30th June 2020. Vol.98. No 12

ISSN: 1992-8645 www.jatit.org E-ISSN: 1817-3195

specificity and sensitivity obtained using cumulative variance of 97% specifically 80PCs as inputs to the ANN-GDX classifier.

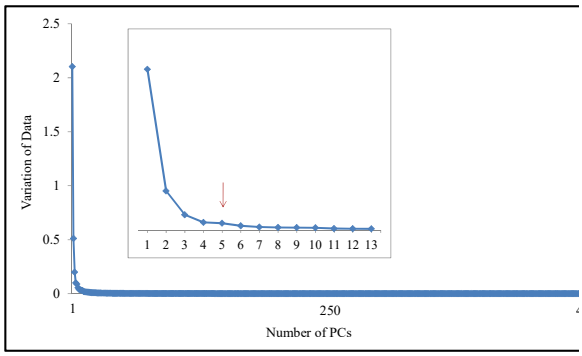

Figure 9: Scree Plot with Stabilization Level of Data

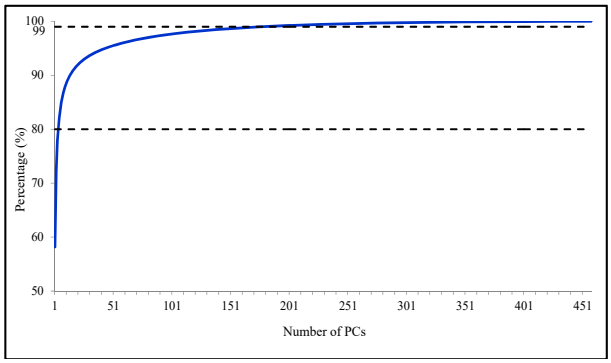

Figure 10: Cumulative Percentage of Variance

5.3 Comparison with Previous Studies

Most studies on human detection were focused on walking pattern [19], [20], [22], [23] that includes intruder detection [18]. It is a challenge to benchmark studies associated to anomalous behavior gait of criminal activities. Thus, Table 6 compares recognition activities on anomalous behavior gait using Kinect body joints. W. Zhang et al. [18] utilized 15 body joints to differentiate walking pattern of householder and intruder. Even though, 94.4% of accuracy was achieved using ANN classifier in classifying the householder and intruder, the recognition was limited using only residence as database. In 2015, D. Nguyen et al. [21] suggested that anomalous behavior gait of human can be recognized by gesture of arm joints for several activities such as beating and changing weapon. Accuracy of 92% was obtained in recognizing 12 gestures with only 9 Kinect body joints using SVM classifier. As for our proposed method, the crime gait pattern for housebreaking crimes done is based on all 20 Kinect body joints in recognizing anomalous behavior at the gate of residential unit with accuracy of 99.78% using ANN classifier. However, poor recognition rate using SVM classifier was due to utilization of whole-body joints in classifying anomalous behavior. Our proposed crime gait pattern eliminates the limit of recognition since the proposed method is applicable at any residential unit with any types of gate.

Table 5: Classification Results of Anomaly Gait based on PCA using ANN and SVM

	PCA		ANN Classifier				SVM Classifier		
			SCG	GDA	GDM	GDX	Linear	RBF	Polynomial
Acc (%)	Cum	97% (80 PCs)	99.35	99.56	87.80	**99.78**	51.20	51.42	49.67
		98% (114 PCs)	**98.48**	**98.48**	78.87	98.04	51.85	51.42	49.02
		99% (177 PCs)	97.82	**98.04**	79.30	**98.04**	51.42	51.42	49.24
	Scree (5 PCs)		91.26	91.07	70.81	**91.94**	51.20	51.85	46.41
	EoC (458 PCs)		**89.98**	53.38	53.60	53.38	52.29	51.42	51.42
Sens (%)	Cum	97% (80 PCs)	99.58	**100**	86.02	**100**	49.76	0	48.28
		98% (114 PCs)	97.03	**97.46**	72.88	97.03	50.46	0	47.39
		99% (177 PCs)	**97.03**	96.61	77.97	96.61	50.0	0	47.55
	Scree (5 PCs)		90.68	91.10	71.61	**92.37**	49.79	100	42.48
	EoC (458 PCs)		**93.22**	79.24	79.24	79.24	53.57	0	0
Spec (%)	Cum	97% (80 PCs)	99.10	99.10	89.69	**99.55**	51.42	51.10	51.10
		98% (114 PCs)	**99.55**	99.55	85.20	99.10	51.42	50.40	50.40
		99% (177 PCs)	98.66	**99.55**	80.72	99.55	51.42	50.59	50.59
	Scree (5 PCs)		**91.93**	91.03	69.96	91.48	52.68	51.64	48.37
	EoC (458 PCs)		86.55	26.01	26.46	26.01	52.11	51.42	51.42

ISSN: 1992-8645 www.jatit.org E-ISSN: 1817-3195

Table 6: Comparison of Previous Studies

Previous Studies	Recognition	Kinect Body Joints	Accuracy (%)	
			ANN	SVM
W. Zhang et al. (2013) [18]	Intrusion detection at residential unit from walking patterns	15 (Excluded head, hand and feet)	94.4	-
D. Nguyen et al. (2015) [21]	Gesture recognition from arm joints	9 (Spine, shoulder, elbow, wrist, hand)	-	**92**
Our Proposed Method: H. Razak et al.	Crime gait pattern from anomalous behavior gait	20	**99.78**	51.42

6. CONCLUSION

As a conclusion, gait recognition approach was proposed in detecting normal and anomalous behavior based on skeleton joints captured by Kinect. Database of normal behavior at residential gate and housebreaking crime behavior was developed in this study. Gait features of behaviors were first defined with high dimensional data of 1400 features from forty joints of X-plane and Y-plane of Kinect. Next, with OLS, gait features were reduced to 840 features. The selection was made according to the high sensitivity of 97.88% and 98.66% of specificity for the twelfth set of OLS. Further, feature optimization was done using PCA has reduced to 80 PCs with higher accuracy of 99.78% and perfect sensitivity in classifying normal and anomalous behavior with ANN-GDX as the best classifier. However, classification results using SVM only yielded approximately 50% accuracy. It is proven that the proposed crime gait pattern worked well for housebreaking crime identification and could further be applied at high security areas such as bank, airports and parking vehicle areas.

Further studies are required using deep learning neural network and to include work in testing the trained classifiers in real-world environment.

ACKNOWLEDGMENTS

This research is funded by Grant No: 600-IRMI/FRGS 5/3 (394/2019), No: FRGS/1/2019/TK04/UITM/01/3 by Ministry of Higher Education (MOHE), Malaysia and Research Management Centre (RMC), Universiti Teknologi MARA (UiTM), Shah Alam, Selangor, Malaysia Grant No: 600-IRMI/MyRA5/3/BESTARI (041/2017). The first author would like to thank Ministry of Education (MOE) Malaysia for the scholarship awarded under MyBrain MyPhD. In addition, special thanks to Royal Malaysia Police for providing legal information and assisting in developing forensic gait features.

REFERENCES:

[1] B. Kröse, T. van Oosterhout, and G. Englebienne, "Video Surveillance for Behaviour Monitoring in Home Health Care," *Proc. Meas. Behav. 2014*, pp. 2–6, 2014.

[2] S. Leixian and Q. Zhang, "Fall Behavior Recognition Based on Deep Learning and Image Processing," *Int. J. Mob. Comput. Multimed.*, vol. 9, no. 4, pp. 1–16, 2019.

[3] W. Min, H. Cui, Q. Han, and F. Zou, "A Scene Recognition and Semantic Analysis Approach to Unhealthy Sitting Posture Detection during Screen-Reading," *Sensors (Basel)*, vol. 18, no. 9, pp. 1–22, 2018.

[4] W. Lawanont, P. Mongkolnam, and C. Nukoolkit, "Smartphone Posture Monitoring System to Prevent Unhealthy Neck Postures," *2015 12th Int. Jt. Conf. Comput. Sci. Softw. Eng. Smartphone*, pp. 331–336, 2015.

[5] M. Sabokrou, M. Fayyaz, M. Fathy, Z. Moayed, and R. Klette, "Deep-Anomaly : Fully Convolutional Neural Network for Fast Anomaly Detection in Crowded Scenes," *J. Comput. Vis. Image Underst. (arXiv00866v2 [cs.CV])*, pp. 1–30, 2018.

[6] B. Delgado, K. Tahboub, and E. J. Delp, "Automatic Detection Of Abnormal Human Events On Train Platforms," *IEEE Natl. Aerosp. Electron. Conf. (NAECON 2014)*, pp. 169–173, 2014.

[7] M. Elhamod and M. D. Levine, "Automated real-time detection of potentially suspicious behavior in public transport areas," *IEEE Trans. Intell. Transp. Syst.*, vol. 14, no. 2,

pp. 688–699, 2013.

[8] Y. Pang, S. Syu, Y. Huang, and B. Chen, "An Advanced Deep Framework for Recognition of Distracted Driving Behaviors," *2018 IEEE 7th Glob. Conf. Consum. Electron.*, pp. 802–803, 2018.

[9] C. Zhang, R. Li, W. Kim, D. Yoon, and P. Patras, "Driver Behavior Recognition via Interwoven Deep Convolutional Neural Nets with Multi-stream Inputs," *arXiv:1811.09128v1 [cs.CV]*, pp. 1–10, 2018.

[10] N. C. Tay, C. Tee, T. S. Ong, K. O. M. Goh, and P. S. Teh, "A Robust Abnormal Behavior Detection Method Using Convolutional Neural Network," in *Alfred R., Lim Y., Ibrahim A., Anthony P. (eds) Computational Science and Technology. Fifth International Conference on Computational Science and Technology. Lecture Notes in Electrical Engineering, Springer, Singapore*, vol. 481, 2019, pp. 37–47.

[11] K. Ko and K. Sim, "Deep convolutional framework for abnormal behavior detection in a smart surveillance system," *Eng. Appl. Artif. Intell.*, vol. 67, pp. 226–234, 2018.

[12] H. Xu, L. Li, M. Fang, and F. Zhang, "Movement Human Actions Recognition Based on Machine Learning," *Int. J. Online Biomed. Eng.*, vol. 14, no. 4, pp. 193–210, 2018.

[13] M. Ben Ayed and M. Abid, "Suspicious behavior detection based on DECOC classifier," *18th Int. Conf. Sci. Tech. Autom. Control Comput. Eng.*, pp. 594–598, 2017.

[14] R. Nar, A. Singal, and P. Kumar, "Abnormal activity detection for bank ATM surveillance," *2016 Int. Conf. Adv. Comput. Commun. Informatics, ICACCI 2016*, pp. 2042–2046, 2016.

[15] Y. Zhu and Z. Wang, "Real-Time Abnormal Behavior Detection in Elevator," in *Zhang Z., Huang K. (eds) Intelligent Visual Surveillance. IVS 2016. Communications in Computer and Information Science, vol 664. Springer, Singapore*, 2016, pp. 154–161.

[16] C. P. Lee, K. M. Lim, and W. L. Woon, "Statistical and entropy based human motion analysis," *2010 2nd Int. Conf. Signal Process. Syst. Stat.*, vol. 1, pp. 734–738, 2010.

[17] M. K. Fiaz and B. Ijaz, "Vision based human activity tracking using artificial neural networks," *2010 Int. Conf. Intell. Adv. Syst. ICIAS 2010*, pp. 1–5, 2010.

[18] W. Zhang and G. Chakraborty, "Construction of intelligent intrusion detection system based on KINECT," *2013 Int. Jt. Conf. Aware. Sci. Technol. Ubi-Media Comput. Can We Realiz. Aware. via Ubi-Media?, iCAST 2013 UMEDIA 2013*, pp. 81–86, 2013.

[19] V. O. Andersson and R. M. Araujo, "Person identification using anthropometric and gait data from kinect sensor," *Proc. Natl. Conf. Artif. Intell.*, vol. 1, pp. 425–431, 2015.

[20] Y. Zha and Y. Fan, "Multi-person gait recognition system based on Kinect," *2016 2nd IEEE Int. Conf. Comput. Commun. ICCC 2016 - Proc.*, pp. 353–357, 2016.

[21] D. D. Nguyen and H. S. Le, "Kinect Gesture Recognition: SVM vs. RVM," *Proc. - 2015 IEEE Int. Conf. Knowl. Syst. Eng. KSE 2015*, pp. 395–400, 2015.

[22] N. Khamsemanan, C. Nattee, and N. Jianwattanapaisarn, "Human Identification from Freestyle Walks using Posture-Based Gait Feature," *IEEE Trans. Inf. Forensics Secur.*, vol. 13, no. 1, pp. 119–128, 2018.

[23] E. M. Owaidah, K. S. Aloufi, and J. H. Alkhatib, "Gait Recognition for Saudi Costume Using Kinect Skeletal Tracking," *2019 2nd Int. Conf. Comput. Appl. Inf. Secur.*, pp. 1–5, 2019.

[24] H. Zhao, Z. Wang, and F. Nie, "Neurocomputing Orthogonal least squares regression for feature extraction," *Neurocomputing*, pp. 1–8, 2016.

[25] C. M. Bishop, "Linear Models for Regression," in *Pattern Recognition and Machine Learning*, 2006, pp. 137–146.

[26] N. Salkind, "Principal Components Analysis," in *Encyclopedia of Research Design*, 2012, pp. 351–367.

[27] M. Mei, "Principal Component Analysis," 2009, pp. 1–9.

[28] Y. Li, Z. Peng, R. Pal, and C. Li, "Potential Active Shooter Detection Based on Radar Micro-Doppler and Range-Doppler Analysis Using Artificial Neural Network," *IEEE Sens. J.*, vol. 19, no. 3, pp. 1052–1063, 2019.

ISSN: 1992-8645 www.jatit.org E-ISSN: 1817-3195

[29] T. Jan, "Neural network based threat assessment for automated visual surveillance," *Proc. 2004 Int. Jt. Conf. Neural Networks*, vol. 2, no. 2, pp. 1309–1312, 2004.

[30] M. Maierdan, K. Watanabe, and S. Maeyama, "Estimation of human behaviors based on human actions using an ANN," *Int. Conf. Control. Autom. Syst.*, no. Iccas, pp. 94–98, 2014.

[31] D. J. Sebald and J. A. Bucklew, "Support vector machine techniques for nonlinear equalization," *IEEE Trans. Signal Process.*, vol. 48, no. 11, pp. 3217–3226, 2000.

[32] Z. Xu, C. Xu, J. Watada, and L. Hu, "A Meta-Heuristic Parameter Selector Based Support Vector Machine for Human Tracking," *2018 Int. Conf. Unconv. Model. Simul. Optim. - Soft Comput. Meta Heuristic, UMSO 2018 - Proc.*, pp. 1–5, 2019.

[33] A. Ouanane, A. Serir, and N. Djelal, "Recognition of Aggressive Human Behavior Based on SURF and SVM," pp. 396–400, 2013.

[34] E. Kita, X. Feng, and H. Shimokubo, "Personal identification by pedestrians behavior," *IEEE Int. Conf. Data Min. Work. ICDMW*, vol. 2017-Novem, pp. 617–624, 2017.

[35] M. Müller, T. Röder, M. Clausen, B. Eberhardt, B. Krüger, and A. Weber, "Documentation mocap database hdm05," *Tech. Rep.*, no. June, 2007.

[36] CMU Graphics Lab, "Carnegie Mellon University Motion Capture Database," *Carnegie Mellon University*. [Online]. Available: http://mocap.cs.cmu.edu/info.php. [Accessed: 09-Aug-2019].

[37] Eyes JAPAN, "mocapdata," *University of Aizu*. [Online]. Available: http://mocapdata.com/Contact.html. [Accessed: 09-Aug-2019].

[38] The Max Planck Society, "Emotional Body Motion Database," *Max Planck Campus, Tübingen, Germany*. [Online]. Available: http://ebmdb.tuebingen.mpg.de/index.php?order_by=duration&last_order=duration. [Accessed: 09-Aug-2019].

[39] SFU MOCAP, "SFU Motion Capture Database," *Simon Fraser University & National University of Singapore*. [Online]. Available: http://mocap.cs.sfu.ca/. [Accessed: 09-Aug-2019].

[40] J. D. Jackson and J. A. Dunlevy, "Orthogonal Least Squares and the Interchangeability of Alternative Proxy Variables in the Social Sciences," *J. R. Stat. Soc. Ser. D (The Stat.*, vol. 37, no. 1, pp. 7–14, 1988.

[41] Z. Gniazdowski, "New Interpretation of Principal Components Analysis," *Zesz. Nauk. WWSI*, vol. 11, no. 16, pp. 43–65, 2017.

[42] P. R. Peres-Neto, D. A. Jackson, and K. M. Somers, "How many principal components? stopping rules for determining the number of non-trivial axes revisited," *Comput. Stat. Data Anal.*, vol. 49, no. 4, pp. 974–997, 2005.